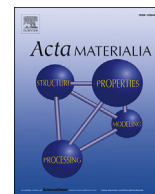




Contents lists available at ScienceDirect

Acta Materialia

journal homepage: www.elsevier.com/locate/actamat

Full length article

Neutron irradiation effects in Fe and Fe-Cr at 300 °C

Wei-Ying Chen ^{a, b, *}, Yinbin Miao ^{a, b}, Jian Gan ^c, Maria A. Okuniewski ^d, Stuart A. Maloy ^e, James F. Stubbins ^a^a University of Illinois at Urbana-Champaign, USA^b Argonne National Laboratory, USA^c Idaho National Laboratory, USA^d Purdue University, USA^e Los Alamos National Laboratory, USA

ARTICLE INFO

Article history:

Received 16 December 2015

Received in revised form

21 March 2016

Accepted 22 March 2016

Available online xxx

Keywords:

Fe-Cr

Neutron

Irradiation

Dislocation loop

Void

Hardness

Orowan

ABSTRACT

Fe and Fe-Cr (Cr = 10–16 at.%) specimens were neutron-irradiated at 300 °C to 0.01, 0.1 and 1 dpa. The TEM observations indicated that the Cr significantly reduced the mobility of dislocation loops and suppressed vacancy clustering, leading to distinct damage microstructures between Fe and Fe-Cr. Irradiation-induced dislocation loops in Fe were heterogeneously observed in the vicinity of grown-in dislocations, whereas the loop distribution observed in Fe-Cr is much more uniform. Voids were observed in the irradiated Fe samples, but not in irradiated Fe-Cr samples. Increasing Cr content in Fe-Cr results in a higher density, and a smaller size of irradiation-induced dislocation loops. Orowan mechanism was used to correlate the observed microstructure and hardening, which showed that the hardening in Fe-Cr can be attributed to the formation of dislocation loops and α' precipitates.

Published by Elsevier Ltd on behalf of Acta Materialia Inc.

1. Introduction

Ferritic-martensitic (F/M) steels are leading candidate materials for fusion reactors and Generation-IV fission reactors [1,2] due to their superior properties such as higher thermal conductivity, lower thermal expansion [2], and their resistance to swelling [3,4], helium embrittlement [5,6] and irradiation creep at high temperatures ($T > 0.4 T_m$) [7]. However, F/M steels exhibit low-temperature ($T < 500$ °C) irradiation-induced embrittlement that leads to a substantial increase in the ductile-to-brittle transition temperature ($\Delta DBTT$) even at very low irradiation doses [8]. It is important to understand the embrittlement mechanism and how it depends on the parameters such as irradiation conditions, composition, etc.

The Cr content of F/M steels is one of the key parameters that determines the irradiation-induced $\Delta DBTT$ [9], swelling [10] and other mechanical properties [11,12]. Remarkably, these properties depend on Cr concentration in a non-monotonic manner. For

$\Delta DBTT$, a minimum was observed at ~10% Cr (in atomic percent, hereafter) [9], leading to the selection of this Cr concentration in many steels proposed for nuclear applications.

Binary Fe-Cr model alloys have been the focus of basic research for studying the effect of Cr on the irradiation embrittlement of F/M steels [11–16]. Those studies showed that the formation of dislocation loops and Cr-rich α' precipitates are the primary hardening mechanisms. It has been shown that the increase of hardening above ~10% Cr can be qualitatively explained with α' phase precipitation [17–19], however it does not explain the increase below ~10% Cr where α' phase is in absence and dislocation loops are the primary source of the embrittlement.

The Cr content affects the dislocation loops as a strengthening mechanism in many aspects. First above all, Cr decreases the mobility of small dislocation loops [20,21], which results in smaller loop sizes and larger loop densities as compared to high purity Fe [11,14,22]. However, the loop size and density are relatively constant beyond ~2% Cr as compared to the significant variation observed for $\Delta DBTT$. In addition, Cr affects the proportion of dislocation loops with $\frac{1}{2}\langle 111 \rangle$ and $\langle 100 \rangle$ Burgers vectors. The $\frac{1}{2}\langle 111 \rangle$ and $\langle 100 \rangle$ loops were suggested to have different

* Corresponding author.

E-mail address: wayneisphil@gmail.com (W.-Y. Chen).

contributions to strength as obstacles to dislocation movements [23]. Also, the two loop types vary significantly in mobility, which lead to different loop morphologies. The Cr dependence of the ratio of two Burgers vectors has been reported previously, but the results were not consistent [11,24].

This paper presents the distinctive microstructural evolution of Fe and Fe-Cr under neutron irradiation at 300 °C. The aim of this present paper is to show the effect of Cr on the process of defect clustering, and to correlate the microstructure with the hardness measurements using the Orowan model.

2. Materials and experimental procedure

2.1. Materials

This study examined neutron irradiation damage in Fe, Fe-10Cr polycrystals and Fe-Cr single crystals. Table 1 shows the chemical composition and grain size of the un-irradiated specimens. The grain size was measured with electron backscatter diffraction (EBSD) [25].

The Fe-10Cr polycrystals were made by Carpenter in Wyomissing, PA. Before irradiation, samples were heated at 980 °C for 30 min, air cooled, then heated at 780 °C for 24 h, and followed by air cooling. The Fe-Cr single crystals were made by Welsch Metallurgy in Cleveland, OH using Czochralski growth aiming at a nominal composition of 14% Cr. The Cr concentration is homogeneous within each specimen, however as shown in Table 2 the Cr concentration varied between specimens due to the evaporation of Cr during the growth process. For clarity, single crystal specimens and polycrystalline specimens are labeled with a SC and a PC, respectively.

2.2. Irradiation

Irradiation was conducted in the Advanced Test Reactor (ATR), Idaho National Laboratory (INL). Specimens with identical irradiation conditions were contained in the same capsule during irradiation. The target irradiation temperature was 300 °C and the target doses were 0.01, 0.1 and 1 dpa. The 0.01 dpa and 0.1 dpa specimens were irradiated in the 'rabbit system' where the capsules were inserted and extracted in the middle of the cycle. The 1 dpa

Table 1
Chemical composition (at%) and grain size of the un-irradiated specimens.

	Fe polycrystals ^a	Fe-10Cr polycrystals ^b	Fe-Cr single crystals ^c
Cr	<0.000002	9.7	13.7
C		0.023	<0.09
Mn	0.00001	<0.01	<0.02
Si	<0.00001	<0.02	
P		<0.009	
S			
Ni	<0.000005		
Mo		<0.06	
Cu	<0.000005	<0.009	
Co			
Al	<0.000005	<0.021	
N		0.006	<0.04
V			<0.02
Ag	<0.000005		
Ca	<0.00008		
Mg	0.000002		
Fe	bal.	bal.	bal.
Grain Size (μm)	2.7	181	–

^a Analysis performed by Goodfellow.

^b Analysis performed by Carpenter.

^c Measured with APT [1].

Table 2
Cr concentrations of Fe-Cr single crystals measured by APT.

	Specimen Label	Irradiation conditions	x _{Cr} (at.%)
Single-Crystals	Fe16Cr-SC	300 °C-1 dpa	16.0
	Fe10Cr-SC	300 °C-0.1 dpa	10.0
	Fe14Cr-SC	300 °C-0.01 dpa	14.0
	Fe14Cr-SC	No irradiation	13.7

specimens were irradiated in standard positions where specimens stayed in the reactor for a complete cycle. As a result, 1 dpa specimens may receive some irradiations at a temperature below target value during reactor power ramping up and down [26].

2.3. Transmission electron microscopy (TEM)

TEM specimens were prepared in the Electron Microscopy Laboratory (EML) at INL and the Low Activation Material Design and Analysis (LAMDA) facility at Oak Ridge National Laboratory (ORNL). Microscopy was performed in the Center for Advanced Energy Studies (CAES), EML and LAMDA facility.

Instead of using the standard 3 mm TEM specimens, this study adopted 2.3 mm specimens in order to reduce the magnetic effect and to save materials. Specimens were mechanically thinned down to around 80 μm, and then jet-polished at –30 to –40 °C to perforation with an electrolyte of 5 vol.% perchloric acid and 95 vol.% methanol. After perforation, specimens were mounted on 3 mm slot grids and then stored in dehydrated ethanol or methanol to reduce oxidation.

TEM was used to observe dislocations, dislocation loops and voids. Dislocations and dislocation loops were imaged under kinematical bright field and centered dark field imaging conditions ($g = 110$ and 200 , $s_g \sim 0.1 \text{ nm}^{-1}$). The dislocation density was estimated using the linear intersect method on the TEM images [27]. The $g \cdot b$ analysis was conducted to determine the Burgers vectors. The habit planes of dislocation loops were determined by observing their inclination planes at the zone axis. The voids were imaged with under- and over-focused imaging conditions.

To obtain the volume density of defects, the foil thickness of the TEM image was estimated primarily with the thickness fringes, and sometimes with convergent beam electron diffraction (CBED) and tilting method if the thickness fringe method was not feasible.

2.4. Hardness measurements

Microhardness was measured in the LAMDA facility with a Vickers diamond hardness indenter. Vickers hardness HV is defined as

$$HV = \frac{F}{A}$$

$$A = \frac{d^2}{2 \sin(68^\circ)}$$

where F is the load in kgf and d is the average of indent diagonals in millimeters. The load and dwell time were 100 g and 15 s, respectively. At least 7 indents were performed for each specimen.

Nanoindentation was performed in CAES in a Hysitron TI-950 TriboIndenter with a high load Berkovich indentation head. A Fixed displacement of 5 μm was used for all measurements. Before indentation, specimens were mechanically polished, and then electro-polished with 5 vol.% perchloric acid in methanol electrolyte for about 10 s to achieve a deformation-free surface. The

Download English Version:

<https://daneshyari.com/en/article/7878445>

Download Persian Version:

<https://daneshyari.com/article/7878445>

[Daneshyari.com](https://daneshyari.com)